Scientific Paper / Artículo Científico

UNIVERSIDAD POLITÉCNICA SALESIANA ECUADOR
INGENIUS
Revista de Ciencia y Tecnología
https://doi.org/10.17163/ings.n34.2025.04
pISSN: 1390-650X / eISSN: 1390-860X

Operative Analysis of Controlled Charging Management for Electric Vehicles: Centralized and Decentralized Coordination

Análisis Operativo de la Gestión de Carga Controlada en Vehículos Eléctricos: Coordinación Centralizada y Descentralizada

Carlos W. Villanueva-Machado[1,*], Jaime E. Luyo[1], Alberto Ríos-Villacorta[2]

Received: 24-07-2024, Received after review: 25-03-2025, Accepted: 23-04-2025, Published: 01-07-2025

Abstract

Electric vehicle (EV) charging management can be implemented through centralized or decentralized strategies. Strategic coordination between these approaches enhances system efficiency and balances energy loads, thereby supporting the widespread adoption of EVs and fostering a sustainable, emissions-free society. In this study, distribution network operators (DNOs), acting as centralized charging managers, are responsible for mitigating the lack of coordination among electric vehicle aggregators (EVAs), which represent decentralized managers. The primary objective of the centralized management in this research is to constrain each decentralized optimization model, characterized using Monte Carlo simulations. Three EV adoption scenarios–comprising 2,000, 2,500, and 3,750 vehicles–are evaluated by comparing decentralized charging management with an unregulated charging baseline in the IEEE 14-bus power system. Improvements are required only in the highest adoption scenario, where the proposed centralized coordination model is applied. The study models energy trading constraints for each EVA, assigning one aggregator per load-bearing bus in the system. Transmission-level results are analyzed and then synthesized for application in the IEEE 13-bus distribution power system. Findings demonstrate that coordinated centralized and decentralized charging management significantly improves operational conditions in both transmission and distribution networks without necessitating changes to travel behavior.

Keywords: Electric Vehicles, Electric Vehicle Aggregators, Monte Carlo Simulation, Optimal Power Flow, Distribution Network Operator, Power System

Resumen

La gestión de la carga controlada de vehículos eléctricos se aplica de forma centralizada y descentralizada. La coordinación estratégica entre ambas optimiza la eficiencia y equilibra la carga de los sistemas energéticos, promoviendo tanto la adopción de vehículos eléctricos, así como una sociedad sostenible y libre de emisiones. Los operadores de las redes de distribución (gestores de carga centralizada) deben controlar la descoordinación entre los agregadores de vehículos eléctricos (gestores descentralizados seleccionados para este estudio). El objetivo de gestión centralizada de esta investigación es acotar cada modelo de optimización descentralizada (caracterizado mediante simulación de Monte Carlo). La gestión descentralizada, se compara con la carga desregulada en el sistema de potencia IEEE de 14 barras para 3 escenarios de adopción de vehículos eléctricos (2000, 2500, 3750 vehículos eléctricos), requiriendo mejoras únicamente en el último escenario, al cual se le aplica la coordinación en gestión centralizada propuesta. El estudio modela las restricciones en la energía comercializada por cada agregador de vehículos eléctricos (uno por barra del sistema eléctrico con carga). Los resultados en transmisión se analizan, sintetizan y aplican al modelo de sistema de potencia de distribución IEEE de 13 barras. Los sistemas de transmisión y distribución de energía coordinan entre la gestión de carga centralizada y descentralizada mejoran las condiciones de operación en los sistemas de potencia sin requerir cambios en los patrones de manejo.

Palabras clave: agregadores de vehículos eléctricos, flujo óptimo de potencia, operador de redes de distribución, simulación Monte Carlo, sistemas eléctricos, vehículos eléctricos

[1,*]Faculty of Mechanical Engineering, Universidad Nacional de Ingeniería, Perú
Corresponding author ✉: cwvillanuevam@uni.pe.

[2]Faculty of Systems Electronics and Industrial Engineering, Universidad Técnica de Ambato, Ecuador

Suggested citation: C. W. Villanueva-Machado, J. E. Luyo and A. Ríos-Villacorta “Operative Analysis of Controlled Charging Management for Electric Vehicles: Centralized and Decentralized Coordination,” *Ingenius, Revista de Ciencia y Tecnología*, N.° 34, pp. 43-60, 2025, DOI: https://doi.org/10.17163/ings.n34.2025.04.

1. Introduction

The increasing adoption of electric vehicles (EVs) has intensified interest in the development of effective charging management strategies. Proper management of EV charging is essential for promoting sustainable electric mobility and reducing reliance on conventional energy sources within power grids.

Previous research [1] has characterized the rise in power system demand caused by EV integration using Monte Carlo simulation. According to that study, distribution network operators (DNOs) must implement centralized electric vehicle charging management (CEVCM) to maintain system stability. Such centralized approaches enable distributed renewable energy sources to meet the additional load imposed by EV charging. In related work, a vehicle-to-grid (V2G) scheduling method has been proposed [2], which incorporates battery protection objectives while utilizing renewable energy in microgrid environments. This approach aims to reduce battery degradation and encourage the use of local renewable generation. Additionally, research by [3] explores the deployment of on-site wind power generation to support EV charging in building-level microgrids. This strategy leverages a Markov decision process and a policy improvement framework based on distributed simulation, demonstrating strong scalability and operational effectiveness.

1.1. Electric Vehicle Charging Optimization

The study presented in [4] highlights the critical role of electric vehicle (EV) charging and discharging management in the context of smart homes and intelligent grids. Similarly, [5] explores the complexity of administering EV charging within smart-home energy management systems. The research conducted in [6] underscores the importance of integrated EV charging management strategies that incorporate enhancements in energy storage infrastructure. In [7], it is emphasized that coordinated interaction between EVs and the grid enables the provision of regulation reserve services while compensating EV owners for battery degradation, thereby reducing overall system operation costs.

Additional studies have proposed frameworks for electric vehicle charge-discharge management (EVCDM). For example, [8] introduces a model utilizing photovoltaic energy outputs to reduce residential energy costs, demonstrating its effectiveness through simulation. In [9], an online coordination method is employed within an EVCDM framework to manage the charging of plug-in electric vehicles (PEVs) in intelligent distribution networks.

Further contributions include [10], which presents a transactive energy framework based on sensitivity analysis to coordinate EV charging with voltage control in low-voltage distribution systems. Complementarily, [11] develops a distributed algorithm for the charging control of plug-in hybrid and electric vehicles. This algorithm eliminates the need for a centralized control unit, increases resilience to single-node or link failures, and scales efficiently with an increasing number of charging points.

Moreover, [12] proposes a peak load management model for scheduling EV charging and discharging based on queuing theory, supported by extensive MATLAB-based simulations. Finally, [13] evaluates a multi-timescale framework under uncertainty conditions, applying a real-time coordinated scheduling method for active distribution networks incorporating-soft open points and PEVs.

1.2. Electric Vehicle Charging Impact on Power Systems

Efficient communication between centralized electric vehicle charging management (CEVCM) and decentralized systems, such as electric vehicle aggregators (EVAs) or parking facilities, is essential for the reliable operation of modern power systems [14]. Similar to the approach in [4], this study addresses the coordination of charging and discharging operations. A 2% increase in NO_x emissions has been observed when communication in decentralized smart charging systems is infrequent, leading to higher operational costs and increased capacity demands on the electrical network. Additionally, study [15] highlights how EVAs influence the pace and pattern of electric vehicle adoption.

Both centralized and decentralized management strategies are necessary to maintain power system stability. Study [16] proposes a coordinated EV management system for low-voltage residential networks, aiming to minimize electricity costs under grid constraints through a multi-agent system architecture. Research [17] supports this objective by reducing energy costs and preventing transformer overloads during EV charging. It introduces the MASCO architecture, which adapts to varying tariff structures using multi-agent, multi-objective reinforcement learning based on energy pricing.

Further contributions include a real-time smart load management (RT-SLM) strategy in [18], which lowers costs and grid losses by incorporating time-varying electricity prices and priority-based charging for plug-in electric vehicles (PEVs). Study [19] suggests a market-based coordination model involving EV owners, fleet operators, and distribution system operators, considering driving needs, costs, and system constraints. Study [20] presents a methodology designed to maximize aggregator profits while maintaining the operational integrity of distribution networks.

Study [21] models EVA participation in both day-ahead and real-time electricity markets, accounting for battery degradation. Similarly, study [22] introduces a demand response program coordinated by aggregators within a reconfigured, grid-connected microgrid, which includes EV charging stations, renewable energy sources, and diesel generators. Building on this line of research, study [23] presents a multi-objective optimization model for managing local multi-energy systems that incorporate PEVs.

Finally, study [24] explores the optimal operation of a grid-connected AC microgrid using stochastic optimization, while study [25] proposes a hybrid decentralized framework that combines robust optimization with stochastic programming to coordinate the management of EVAs and energy hubs under uncertainty.

1.3. Electric Vehicle Adoption Analysis

According to [26], electric vehicle (EV) sales data from 2022 show that China leads the global EV market. In Latin America, reference [27] identifies three primary categories of EV incentives implemented in 2019: purchase incentives, use and circulation incentives, and other promotional measures. Reference [28] notes that several Latin American countries exhibit high levels of EV imports, while [29] reports the number of EV chargers available by country.

Figure 1 summarizes this information, indicating an average global growth of 17% in EV adoption. North America experienced a 46% year-over-year increase, while other regions recorded an 81% rise compared to the previous year. On a global scale, the COVID-19 pandemic temporarily slowed the growth of EV and hybrid vehicle adoption, with recovery progressing gradually through 2023. Brazil, Mexico, and Colombia are currently increasing their rates of EV importation. The average ratio of electric vehicles per charging station is 18.75, with these stations distributed throughout power systems.

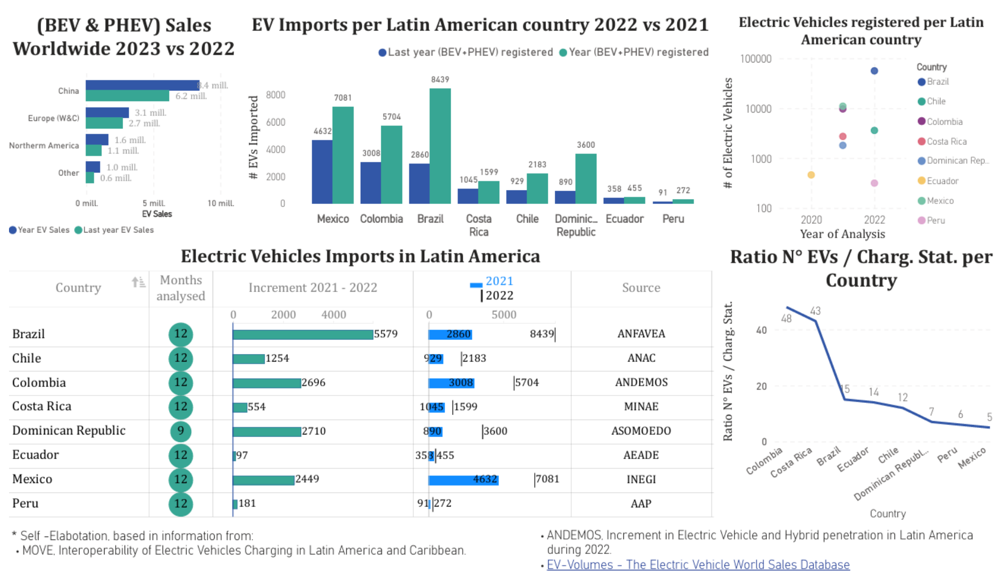

Figure 1. Adoption of Electric Vehicles worldwide and in LA

As noted in [30], the Peruvian Ministry of Energy and Mining issued a decree in August 2019 to promote the adoption of EVs and plug-in electric vehicles (PEVs). Reference [1] presents a Monte Carlo simulation analysis featuring three scenarios and two output variables, designed to characterize the stochastic behavior of EVs. These scenarios assess the operation of EVAs under conditions that do not adversely affect power system performance.

2. Materials and Methods

Figure 2 presents the flow diagram of the methodology employed in this research. The process begins with a Monte Carlo Simulation (MCS), which characterizes the geographic distribution and travel behavior of electric vehicle (EV) owners. These MCS-generated scenarios are then modeled within a decentralized electric vehicle charging management (DEVCM) framework. The outputs from the DEVCM model subsequently trigger a centralized electric vehicle charging management (CEVCM) analysis, evaluating its impact on the operation of the distribution network (DN). Based on this evaluation, modifications are introduced into the DEVCM model by incorporating coordination constraints between the decentralized and centralized charging strategies. The coordinated charging strategy is then tested on a distribution power system using the IEEE 13-bus network, as illustrated in Figure 3. The dataset used in this study is available at the following repository [31].

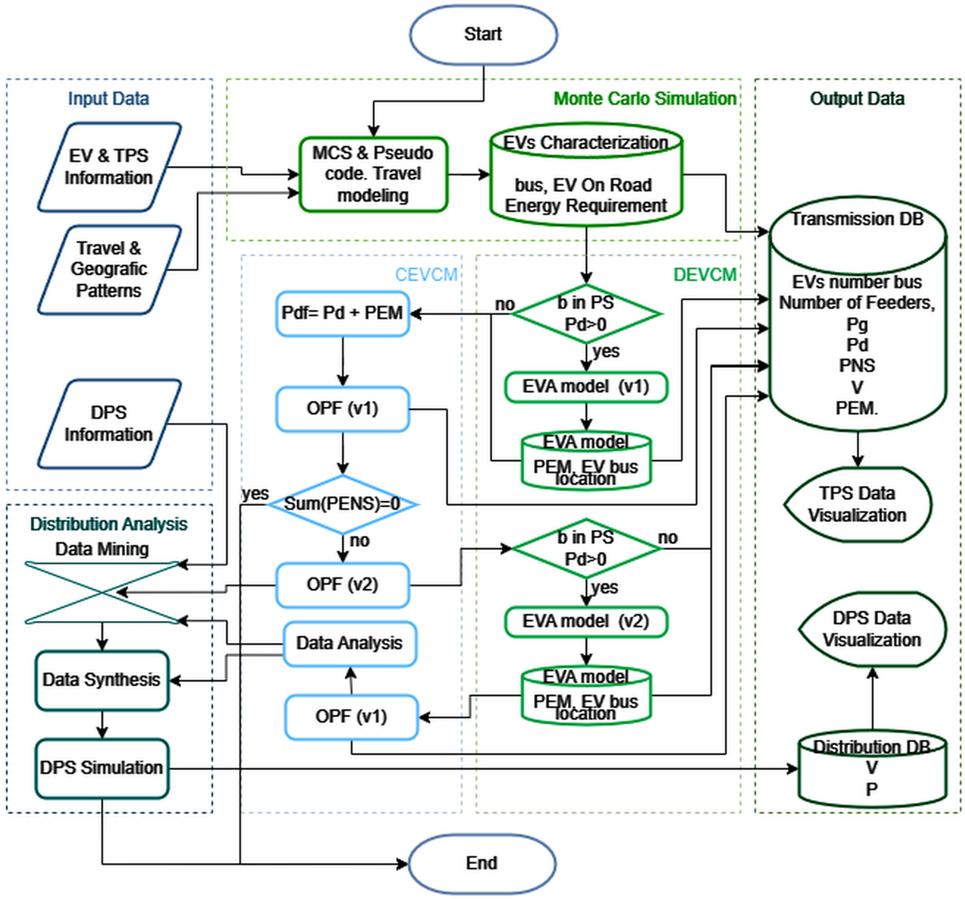

Figure 2. Method used by each EV adoption scenario

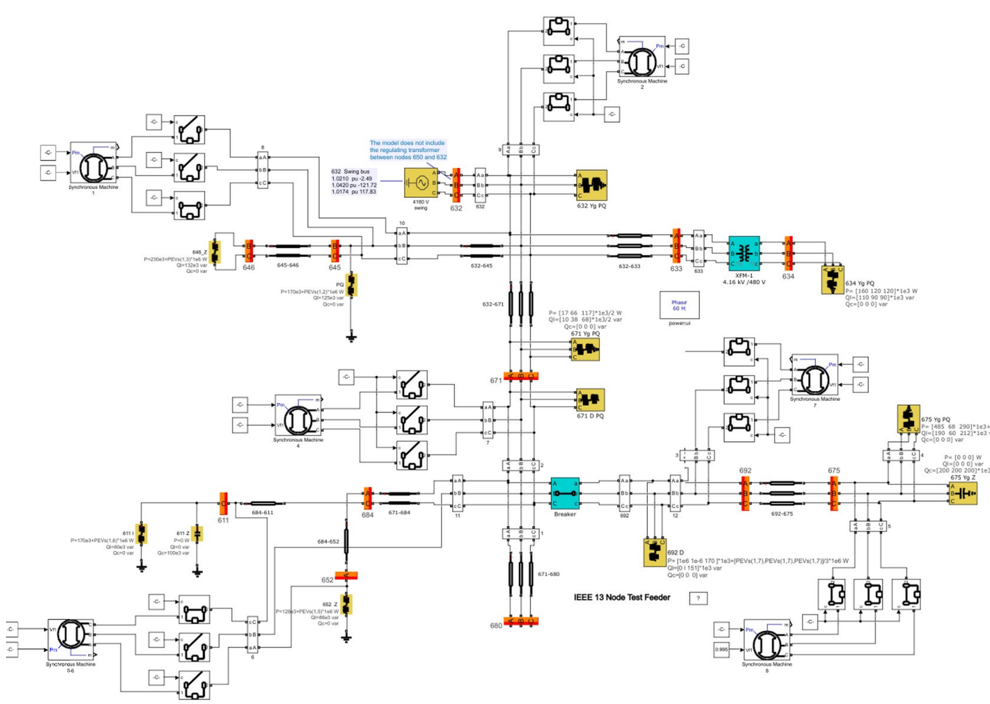

Figure 3. Distribution Power System (IEEE 13 bus) simulation

2.1. Scenario analysis and inputs

Following the approach in [1], this methodology models the stochastic behavior of electric vehicle (EV) charging. Reference [1] presents a centralized electric vehicle charging management (CEVCM) model applied in Peru across three scenarios. The present study builds upon that framework, comparing the same three scenarios involving 2,000, 2,500, and 3,750 EVs under controlled charging conditions. The primary objective of this research is to identify the coordination infrastructure required between decentralized (DEVCM) and centralized (CEVCM) charging management systems. Each scenario is evaluated using Monte Carlo Simulation to characterize the EVs' energy requirements. For each case, the simulation produces minimum and maximum output values, denoted as s_{min} and s_{max}. respectively.

2.2. Monte Carlo Simulation

The study defines the departure and arrival points for each electric vehicle (EV) based on the EV aggregator (EVA) closest to the user's home and workplace. Table 1 reports the number of EVs assigned to each bus for both references–departure (Dep.) and arrival (Arr.)–as illustrated in Figure 4(a).

Previous studies have characterized EV travel patterns, such as the work in [32], which describes departure behavior, and [33], which presents arrival conditions for a subset of EV users. Figure 4(b)presents the probability distribution functions for home departure and arrival times. Accordingly, this research adopts normal distributions to model these stochastic variables, maintaining neutrality with respect to specific driving behavior policies.

Figure 4(c) draws from [1] to characterize regional travel patterns by categorizing trips into high-, medium-, and low-speed segments. The probabilistic characteristics of each speed category are shown in Figure 4(d). Together, these figures represent the stochastic modeling of the geographic variables used in this study.

Table 1. Geographical Distribution of EVs by Bus, Scenario, and Monte Carlo Simulation (MCS) Output

	Scenario 1				Scenario 2				Scenario 3			
EVs	minimum		maximum		minimum		maximum		minimum		maximum	
Bar	Dep.	Arr.	Dep.	Arr.	Dep.	Arr.	Dep.	Arr.	Dep.	Arr.	Dep.	Arr.
2	201	187	174	190	251	281	96	262	461	449	316	375
3	179	174	137	155	183	100	183	55	260	262	296	285
4	310	304	146	111	256	458	199	154	427	594	271	305
5	177	202	89	90	372	223	111	118	571	414	214	132
6	203	221	325	201	229	274	193	339	341	285	324	562
9	223	219	178	105	244	240	176	258	388	380	331	370
10	210	270	74	104	285	283	217	229	403	473	257	243
11	163	123	129	140	156	237	277	195	285	197	344	299
12	70	124	190	287	171	91	282	170	236	132	438	309
13	180	127	246	396	206	236	272	486	161	445	426	441
14	84	49	312	221	147	77	494	234	217	119	533	429

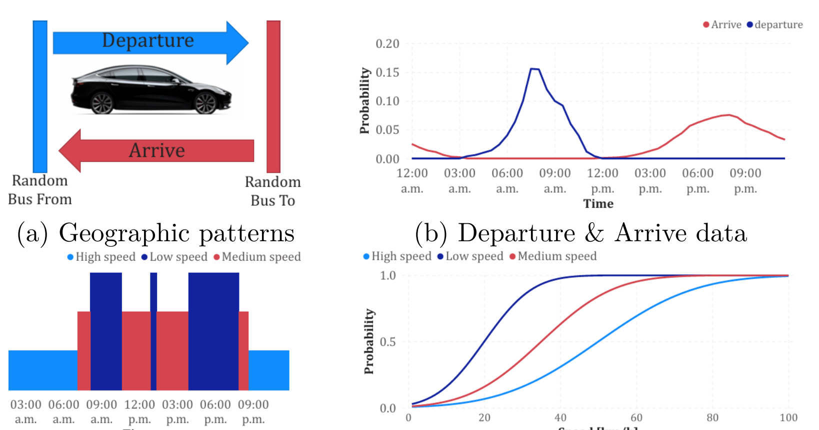

(a) Geographic patterns (b) Departure & Arrive data

(c) Daily Traffic Speed (d) Cumulative Density Function of Speed

Figure 4. Electric vehicle behavior patterns

These stochastic variables define the departure times $\mathrm{dep_{v,s}}$, arrival times $\mathrm{arr_{v,s}}$, travel distance $td_{\mathrm{v,s}}$ and speed during the analyzed period $\mathrm{sv_{t,v,s}}$. In addition to this data, the methodology requires information about the energy exchanged between electric vehicles and their assigned EVA. Accordingly, the trip modeling presented in Figure 5 and detailed in Section 2.2.1, Pseudo Trip Modeling Code, incorporates a specific energy consumption variable $\mathrm{SC_{v,s}}$ expressed in kilowatt-hours per kilometer [kWh/km].

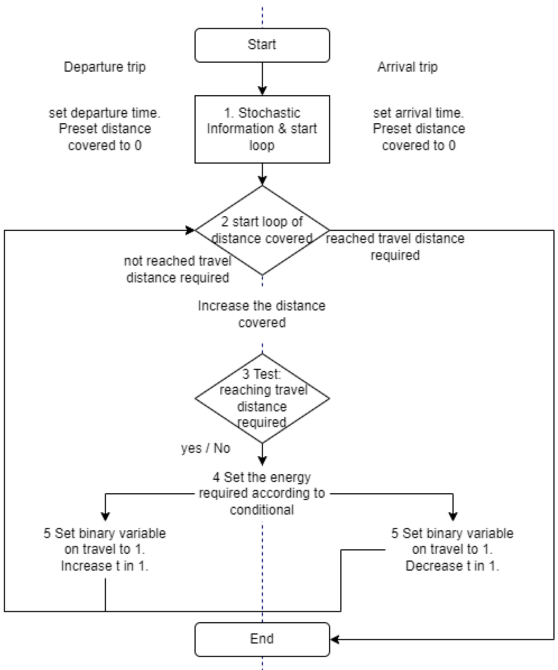

Figure 5. Trip Modeling

2.2.1. Pseudo code: trip modeling

1. 2. Initialize departure and arrival times, along with the time variable fordistance covered. $t = \mathrm{dep}_{v,s} \wedge \mathrm{rdt}_{v,s} = 0$ for the departure trip and $t = \mathrm{arr}_{v,s} \wedge \mathrm{rdt}_{v,s} = 0$ for the return trip.

2. Begin loop to accumulate distance traveled until the total trip distance is reached:

$$while \mathrm{rdt}_{v,s} \leq td_{v,s}$$

$$rdt_{v,s} = rdt_{v,s} + sv_{v,s} \times \frac{24}{T}$$

3. Evaluate the conditional statement to determine whether the final travel period has been reached–that is, whether the trip distance has been fully covered–and compute the energy required by the electric vehicle during travel:

$$if rdt_{v,s} \leq td_{v,s}$$

$$R_{t,v,s} = \frac{sv_{v,s} \times SC_{v,s}}{n_{dsg}} \times \frac{24}{T}$$

4. Assign the energy demand required for the final segment of the trip, based on the remaining distance to be traveled:

$$else \left\{ R_{t,v,s} = (sv_{v,s} + td_{v,s} - rdt_{v,s}) \times \frac{SC_{v,s}}{n_{dsg}} \right\}$$

5. Assign the final departure time and initial arrival time, along with the binary variable representing the in-route state of the trip:

$$X_{t,v,s} = 1 \wedge t = +1 \Rightarrow \mathrm{de}_{v,s} = t \quad \text{(for dep. trip)}$$

$$X_{t,v,s} = 1 \wedge t = -1 \Rightarrow \mathrm{ai}_{v,s} = t \quad \text{(for arr. trip)}$$

2.2.2. MCS outputs

Once the trip is modeled, the binary variable$CS_{b,t,v,s}$ is used to assign each electric vehicle to a specific bus within the system. This variable also tracks the vehicle's charging stage on an hourly basis, enabling the corresponding EVA to collect energy demand information from all vehicles within its assigned area. The definitions and calculations for this variable are provided in equations(1) and (2).

$$CS_{Fr_{v,s},\, t,\, v,\, s} = 1 \quad \forall \; arr_{v,s} < t < dep_{v,s} \qquad (1)$$

$$CS_{To_{v,s},\, t,\, v,\, s} = 1 \quad \forall \; de_{v,s} \leq t \leq ai_{v,s} \qquad (2)$$

To characterize the daily charging requirements of electric vehicles (EVs), the Monte Carlo Simulation (MCS) process performs 1,000,000 micro-stochastic evaluations, comprising 200 samples of 2,000 EVs, 120 samples of 2,500 EVs, and 80 samples of 3,750 EVs. These evaluations correspond to three predefined scenarios. The MCS results provide aggregate system-level charging data, which serve as input for the decentralized charging management strategy.

The simulation aggregates the total energy required by all EVs under analysis, denoted as $GChR_s$, and allows for comparative analysis across the sampled scenarios. Equation (3) defines this cumulative energy requirement during travel. For each scenario, the MCS also identifies the minimum and maximum samples, denoted ass_{min} and s_{max} respectively.

$$GChR_s = \sum_v \sum_t R_{t,v,s} \qquad (3)$$

2.3. Decentralized electric vehicle charging management

The methodology applies decentralized electric vehicle charging management (DEVCM) modeling through EV aggregators (EVAs) at each bus where feeder integration is permitted. This study models the interaction at aggregator busk, assuming that the EVAs involved (corresponding to the "from" and "to" buses) are owned by different entities. The model uses the variables $CS_{k,t,v,s}$ and $R_{t,v,s}$ to determine the location and energy demand of each electric vehicleover time.

The methodology incorporates the model proposed in [21], adapting it to account for uncertainty in EV departure and arrival times. While the departure and arrival locations remain fixed, the associated time variables are modified, as illustrated by the probability distributions in Figure 4(b) . Specifically, departure times are modeled using a normal distribution with a mean of 08:02 and a standard deviation of 01:11, while arrival times follow a normal distribution with a mean of 22:04 and a standard deviation of 04:18.

This study analyses a set of samples $s \in S$, as described in Section 2.2.1 (Pseudo Trip Modeling Code). In this case, the distance traveled $td_{v,s}$ remains unchanged, while only the departurede $p_{v,s}$ and arrival $arr_{v,s}$. At this stage, the sets ,used for the Monte Carlo simulation, is limited to its minimum and maximum output cases. During DEVCM optimization, the set $n \in N$ represents the samples used for real-time operation. Each sample is assigned an equal probability of occurrence $\pi_n = \frac{1}{N}$, reflecting the absence of historical data and the neutrality of policy assumptions. Finally, in line with the objectives of this study, the energy traded through EVAs must be regulated to ensure coordination and maintain power system (PS) capacity.

For this research, the parameter P_t^{SYScap} represents the upper bound of the total charging demand permitted within the power system. This constraint accounts for the aggregate energy traded in both the day-ahead (DA) and real-time (RT) electricity markets. As shown inequation (4), its initial value corresponds to the sum of power demands across all buses at the system's annual peak load hour:

$$P^{SYScap} = \sum_b Pd_b \tag{4}$$

The DEVCM formulation is primarily based on the model presented in [21]; however, this study refines the approach by modifying several constraints–specifically equations (7), (8), (10), (11), (14), (18), (20), (22), (23) and (24). Furthermore, equations (25) through (42) adapt the algorithm by transforming the original nonlinear model into a mixed-integer linear programming (MILP) formulation. A comprehensive terminology section follows the mathematical formulation, describing all sets, parameters, and variables used in the model.

$$\min C = DAEM - RTEM^{\downarrow} + RTEM^{\uparrow} + BATCOST \tag{5}$$

$$\text{DAEM} = \Delta t \sum_t^T \lambda_t \times P_t^{EM} \tag{6}$$

$$\text{RTEM}^{\uparrow} = \Delta t \sum_t^T \sum_n^N \pi_n \times \lambda_{t,n}^{\uparrow} \times P_{t,n}^{-} \tag{7}$$

$$\text{RTEM}^{\downarrow} = \Delta t \sum_t^T \sum_n^N \pi_n \times \lambda_{t,n}^{\downarrow} \times P_{t,n}^{+} \tag{8}$$

$$\text{BATCOST} = BC^{ES} \times \sum_t^T \sum_v^V \sum_n^N \frac{m_v}{100} \times \frac{soc_{t,v,n}^{deg}}{BC_v^{ES}} \times C_v^{ES} \tag{9}$$

$$0 \leq P_{t,n}^{+} + P_{t,n}^{-} \leq \sum_v^V P_{t,v,n}^{B2G} \times \eta^{dsg} \tag{10}$$

$$\sum_n^N \left(P_{t,n}^{-} - P_{t,n}^{+}\right) = 0 \tag{11}$$

$$\begin{aligned} P_t^{EM} = &\sum_v^V \left(P_{t,v,n}^{G2B} - P_{t,v,n}^{B2G} \times \eta^{dsg}\right) \times CS_{k,t,v,s} \\ &+ P_{t,n}^{+} - P_{t,n}^{-} \quad \forall t \in T \wedge n \in N \end{aligned} \tag{12}$$

$$P_{t,v,n}^{B2R} \times \eta^{dsg} = R_{t,v,n} \tag{13}$$

$$0 \leq P_{t,v,n}^{G2B} + P_{t,v,n}^{B2G} \leq P^{max} \times CS_{k,t,v,s} \tag{14}$$

$$0 \leq P_{t,v,n}^{B2R} \leq P^{max} \times X_{t,v,n} \tag{15}$$

$$0 \leq P_{t,v,n}^{G2B}, \quad 0 \leq P_{t,v,n}^{B2G} \tag{16}$$

$$\begin{aligned} soc_{t,v,n} = soc_{t-1,v,n} + \Delta t \times \Big(&P_{t,v,n}^{G2B} \cdot n^{chg} \\ &- P_{t,v,n}^{B2G} - P_{t,v,n}^{B2R}\Big) \end{aligned} \tag{17}$$

$$\begin{aligned} soc_{1,v,n} = soc_{T,v,n} + \Delta t \times (&P_{1,v,n}^{G2B} \cdot n^{chg} \\ &- P_{1,v,n}^{B2G} - P_{1,v,n}^{B2R}) \end{aligned} \tag{18}$$

$$0 \leq \underline{SoC} \leq soc_{t,v,n} \leq \overline{SoC} \leq BC^{ES} \tag{19}$$

$$soc_{t=1} = SoC_{n,v}^{init} \tag{20}$$

$$soc_{t,v,n}^{deg} \times CS_{k,t,v,s} \geq soc_{t-1,v,n} \times CS_{k,t,v,s} - soc_{t,v,n} \times CS_{k,t,v,s} \quad (21)$$

$$DAEM = \Delta t \sum_{t=1}^{T} \sum_{b=1}^{B} (\lambda_b - \lambda_{b-1}) \times \left(P_{t,b}^{EMefective} \right) \quad (22)$$

$$RTEM^{\uparrow} = \Delta t \sum_{t=1}^{T} \sum_{s=1}^{S} \sum_{b=1}^{B} \pi_n \times (\lambda_b - \lambda_{b-1}) \times \left(P_{t,n,b}^{-efective} \right) \quad (23)$$

$$RTEM^{\downarrow} = \Delta t \sum_{t=1}^{T} \sum_{s=1}^{S} \sum_{b=1}^{B} \pi_n \times (\lambda_b - \lambda_{b-1}) \times \left(P_{t,n,b}^{+efective} \right) \quad (24)$$

$$P_t^{EM} = P_t^{EM+} - P_t^{EM-} \quad (25)$$

$$P_{t,b}^{EMefective} = P_{t,b}^{EMefective+} - P_{t,b}^{EMefective-} \quad (26)$$

$$P_t^{EM} + P_t^{Sys} \geq P_{b-1}^{PQP} \times PQP_{t,b} \quad (27)$$

$$P_t^{EM} + P_{t,n}^{-} - P_{t,n}^{+} + P_t^{Sys} \geq P_{b-1}^{PQP} \times PQP_{t,n,b}^{n} \quad (28)$$

$$P_t^{EM} + P_t^{Sys} \leq P^{SYScap} \quad (29)$$

$$P_t^{EM} + P_{t,n}^{-} - P_{t,n}^{+} + P_t^{Sys} \leq P^{SYScap} \quad (30)$$

$$P_{t,b}^{EMefect+} \geq P_t^{EM+} - M_{big} \times (1 - PQP_{t,b}) \quad (31)$$

$$P_{t,b}^{EMefect+} \leq P_t^{EM+} \quad (32)$$

$$P_{t,b}^{EMefect+} \leq M_{big} \times (1 - PQP_{t,b}) \quad (33)$$

$$P_{t,b}^{EMefect-} \geq P_t^{EM-} - M_{big} \times (1 - PQP_{t,b}) \quad (34)$$

$$P_{t,b}^{EMefect-} \leq P_t^{EM-} \quad (35)$$

$$P_{t,b}^{EMefect-} \leq M_{big} \times (1 - PQP_{t,b}) \quad (36)$$

$$P_{t,n,b}^{+efect} \geq P_{t,n}^{+} - M_{big} \times \left(1 - PQP_{t,n,b}^{n}\right) \quad (37)$$

$$P_{t,n,b}^{+\text{efect}} \leq P_{t,n}^{+} \quad (38)$$

$$P_{t,n,b}^{+efect} \leq M_{big} \times (1 - PQP_{t,n,b}^{n}) \quad (39)$$

$$P_{t,n,b}^{-efect} \geq P_{t,n}^{-} - M_{big} \times (1 - PQP_{t,n,b}^{n}) \quad (40)$$

$$P_{t,n,b}^{-efect} \leq P_{t,n}^{-} \quad (41)$$

$$P_{t,n,b}^{-efect} \leq M_{big} \times (1 - PQP_{t,n,b}^{n}) \quad (42)$$

Terminology:

Symbol	**Description**
C	Total cost associated with the Electric Vehicle Aggregator (EVA)
$DAEM$	Cost of energy purchased in the day-ahead electricity market (DA)
$RTEM$	Cost of energy traded in the real-time electricity market (RT)
$BATCOST$	Cost associated with battery lifetime degradation (TVB)
Sets, Universe	
n, N	Samples analyzed
t, T	Time
v, V	Electric vehicles
b, B	PQP probability steps
$\downarrow$	Surplus energy (energy available for sale)
$\uparrow$	Deficit energy (energy required for purchase)
Variables and Parameters	
$\lambda_t, \lambda_{t,s}^{\uparrow}, \lambda_{t,s}^{\downarrow}$	Unit prices of energy in the DA and RT markets
P_t^{EM}	Power traded in the DA electricity market
$P_{t,s}^{-}, P_{t,s}^{+}$	Power deficit and surplus traded in the RT market
m_v	Linear degradation rate associated with battery lifetime
C_v^{ES}	Cost of energy storage [$/kWh]
BC_v^{ES}	Energy storage capacity
$soc_{t,v,n}^{deg}$	Battery degradation equivalent to state of charge
n^{chg}	Battery charging efficiency
n^{dsg}	Battery discharging efficiency
$P_{t,v,n}^{B2G}$	Power fed from the battery to the grid
$P_{t,v,n}^{G2B}$	Power fed from the grid to the battery
$P_{t,v,n}^{B2R}$	Battery power used during the trip
$R_{t,v,n}$	Energy consumption during the trip [kWh]
$X_{t,v,n}$	Binary variable indicating travel state
$P^{\max}$	Maximum allowed charging power

Symbol	Description
$P^{\max}$	Maximum allowed charging power
$\underline{SoC}$	Lower bound of the battery state of charge
$\overline{SoC}$	Upper bound of the battery state of charge
$SoC_{n,v}^{\text{init}}$	Initial battery state of charge (randomly assigned)
$P_{t,b}^{EMefect}$	Effective DA power for step b
$P_{t,n,b}^{-efect}$	Effective power deficit for step b
$P_{t,n,b}^{+efect}$	Effective power surplus for step b
$PQP_{t,b}$	Binary indicating whether total DA load $\leq P_b$
$PQP_{t,n,b}^{n}$	Binary indicating whether total RT load $\leq P_b$
M_{big}	Parameter used for algorithm constraints

The DEVCM incorporates these constraints to optimize its economic variables. As a result, each EVA reports to the distribution network operator (DNO) the required power $P_{k,t,s}^{EM}$ at busk during each periodt for the two representative scenarios: s_{min} and s_{max}. The DNO processes this informationas detailed in the following sections. Due to the computational complexity of the DEVCM, the decentralized electric vehicle charging models were executed using the NEOS Server, as supported by [34–36], for each load-carrying bus.

2.3.1. Electric vehicle aggregator data

The vehicle data used in this study is based on the Tesla Model 3, as reported in [21]. The specific energy consumption ranges between <0.19;0.25> kWh/km, and the battery capacity is BCES=80kWh. The battery degradation cost is defined as $C_v^{ES} =< 100 - 140 >$ MWh, and the linear approximation of battery lifetime is $m_v =< 0.0006, 0.0017 >$.

In addition, information related to the EVA charging stations includes a maximum charging power of $P_{max} = 150$ KW, with both charging and discharging efficiencies set at $n_{chg} = 90$ % and $n_{dsg} = 90$ %, respectively The state-of-charge (SoC) operating limits, as recommended by the manufacturer, range from 15% to 95%.

2.4. Centralized electric vehicle charging management

The centralized electric vehicle charging management (CEVCM) is formulated as an optimal power flow (OPF) problem that processes the aggregated power requests $P_{k,t}^{EM}$ collected from all network EV aggregators. This information modifies the day-ahead load planning of the power system. Equation (43) represents the impact of each aggregator on the system load: if electric vehicles require energy, the load increases; conversely, if the EVs inject energy into the power system ($P_{k,t}^{EM}$ with negative value), the load decreases accordingly.

$$Pd_{k,t,s} = Pdps_{k,t,s} + P_{k,t,s}^{EM} \quad \forall s \in \{s_{\min}, s_{\max}\} \tag{43}$$

The study in [1] presents a CEVCM model, which is refined in the present research. Both models rely on power flow analysis to ensure proper power system (PS) operation, incorporating a contingency variable and various types of constraints. For each period t , the CEVCM is modeled using the following equations. Equation (44) defines the objective function, which minimizes power losses and penalizes non-supplied energy (NSE). The equality constraints, represented by ($h(x) = 0$), are described in equations (45) through (48). Equation (49) introduces the inequality constraint $g(x)$ ($g(x) < 0$). Finally, equations (50) through (53) define the bounds on the control variables, expressed as ($\underline{x} < x < \overline{x}$). All of these equations are applied to each time interval analyzed.

$$of = \sum_{k=1}^{n_{bus}} (C_{pen} \cdot NSE_k) + Pg_{slack} \tag{44}$$

$$Pg_k + NSP_k = Pd_k + \sum_{m=1}^{n_{bus}} P_{km} \tag{45}$$

$$Qg_k = Qd_k + Qsh_k + \sum_{m=1}^{n_{bus}} Q_{km} \tag{46}$$

$$P_{km} = V_k V_m Y_{km} \cos(\theta_{km} + \delta_{km}) - V_k^2 \cos(\tau_{km}) \tag{47}$$

$$Q_{km} = -V_k V_m Y_{km} \sin(\theta_{km} + \delta_{km}) + V_k^2 Y_{km} \sin(\tau_{km}) \tag{48}$$

$$S_{km} = \sqrt{P_{km}^2 + Q_{km}^2} \leq S_{km}^{up} \tag{49}$$

$$V_i^{low} \leq V_i \leq V_i^{up} \tag{50}$$

$$d_i^{low} \leq d_i \leq d_i^{up} \tag{51}$$

$$P_{g_i}^{low} \leq P_{g_i} \leq P_{g_i}^{up} \tag{52}$$

$$Q_{g_i}^{low} \leq Q_{g_i} \leq Q_{g_i}^{up} \tag{53}$$

Terminology:

Symbol	**Description**
OPF	Optimal Power Flow
NSE	Not Supplied Energy
PS	Power System
NSP	Not Supplied Power
low	Lower limit
up	Upper limit
Subscripts, Universe	
b, nbus	Bar in the power system (also: i, j, k, m)
Variables and Parameters	
$Pdps_i$	PS initial active power demand parameter
Pd_i	Active power demand
Qd_i	Reactive power demand
Pg_i	Active power generation
Qg_i	Reactive power generation
P_{ij}	Active power flow from bus i to j
Q_{ij}	Reactive power flow from bus i to j
S_{ij}	Apparent power flow from bus i to j
V_i	Voltage magnitude
δ_{km}	Voltage angle difference between buses k and m
Y_{km}	Admittance matrix magnitude
θ_{km}	Admittance matrix angle

The application results indicate that some scenarios exhibit the presence of not supplied power (NSP). Consequently, CEVCM operators must regulate the exchange of information with the DEVCM in order to adjust the energy traded in the day-ahead (DA) electricity market. When the load exceeds the available power system (PS) capacity, distribution network operators (DNOs) activate the load limit calculation for the EVAs associated with the affected buses. For further details, refer to Section 3. Results and Discussion.

2.4.1. Coordination between centralized and decentralized Charging Management

EV aggregators (EVAs) must apply a predefined limit when energy is requested from the power system. To quantify this limit, distribution network operators (DNOs) incorporate an additional variable into their optimization model: $P_{cap,k}^{EM}$, representing the energy trading capacity. This variable functions similarly to the NSE variable, regulating the maximum amount of power that EVAs are allowed to request from the system. Accordingly, this model modifies equation (45) by replacing it with equation (54), which restricts the value of the energy traded by EVAs in relation to the final demand of the power system, as defined in equation (55).

$$Pg_k + NSP_k = Pd_k + P_{cap,k}^{EM} + \sum_m P_{km} \tag{54}$$

$$P_{cap,k}^{EM} \leq Pd_k \tag{55}$$

EVAs must update their models, specifically equations (29) and (30), by adjusting the corresponding constraints based on temporary data provided by the regulatory agent for each EVA. Accordingly, the model adopts the modified formulations given by equations(56) and (57).

$$P_t^{EM} \leq P_{cap}^{EM} \tag{56}$$

$$P_t^{EM} + P_{t,n}^{-} - P_{t,n}^{+} \leq P_{cap}^{EM} \tag{57}$$

2.4.2. Transmission power system analyzed

The transmission power system analyzed in this study is based on the IEEE 14-bus model, as presented in [37]. Additionally, power factor data from the SEIN system, as reported by COES-SINAC, was used to adapt the model for daily analysis. This data corresponds to weekdays (Monday through Friday) in February 2020, prior to the national impact of the SARS-CoV-19 outbreak, which began affecting the country in March 2020. The reference day for peak load conditions is February 19, 2020.

2.4.3. Distribution analysis

In addition to the transmission system analysis, this study evaluates the distribution network using the IEEE 13-bus power system. Figure 3 illustrates the layout of this distribution system. The distribution analysis incorporates outputs from the transmission-level simulation, including bus voltages and load requirements. To generate representative distribution-level data, a data mining process is applied, which uses a stochastic characterization of the transmission results. This is achieved through a Monte Carlo simulation, which produces statistical samples based on the transmission system outputs.

In Figure 3, the presence of generators simulates vehicle-to-grid (V2G) energy injections from electric vehicles at different buses in the distribution system. The high-voltage side of the main transformer is not modeled, as its primary role is voltage regulation, which could interfere with the objective of monitoring voltage behavior within the distribution network. Following the data analysis and mining process, the distribution analysis includes a data synthesis stage. This stage produces a variety of statistical samples that synthetically represent the behavior of the distribution network under the influence of V2G technology and the power demand imposed by EV aggregators (EVAs).

3. Results and Discussion

Research in [1] presents a CEVCM model applied to the Peruvian context under three adoption scenarios. Building upon that framework, this study explores the coordination infrastructure between decentralized (DEVCM) and centralized (CEVCM) electric vehicle charging management models by comparing the same three scenarios.

3.1. Decentralized Electric Vehicle Charging Management

The distribution network operator (DNO) requires the amount of energy to be traded in each period of the day-ahead (DA) market. Table 2 presents the total daily energy traded for each scenario, including the minimum and maximum outputs obtained from the Monte Carlo Simulation (MCS) analysis.

Figure 6 (a) displays the minimum MCS outputs, while Figure 6 (b) illustrates the maximum outputs. According to Table 2, the EVAs associated with buses 6, 9, 12, 13, and 14 cause deviations in scenarios 2 and 3.

The electric vehicle characterization conducted in this study enables future analysis of regulatory measures focused on travel behavior and geographic distribution. Study [5] also considers uncertainties related to power generation, load demand, and real-time electricity pricing; however, its analysis is limited to a typical residential household.

Table 2. Daily energy traded with the power system by EVA

PEM [MWh]	Scenario 1		Scenario 2		Scenario 3	
Bar	minimum	maximum	minimum	maximum	minimum	maximum
2	2.211	2.188	2.953	2.103	4.802	3.887
3	2.022	1.806	1.768	1.504	2.926	3.308
4	2.469	1.293	2.321	1.566	3.313	2.361
5	1.384	0.936	1.735	1.002	3.144	1.290
6	2.502	3.357	2.835	3.389	60.494	5.655
9	1.849	2.147	2.083	2.795	3.061	59.141
10	1.809	1.101	2.255	2.150	3.265	2.422
11	1.859	1.758	2.417	2.848	2.849	3.777
12	1.526	3.381	1.930	50.309	40.676	5.078
13	1.870	1.758	2.713	61.462	44.124	79.022
14	1.392	3.381	2.192	6.734	39.120	8.427

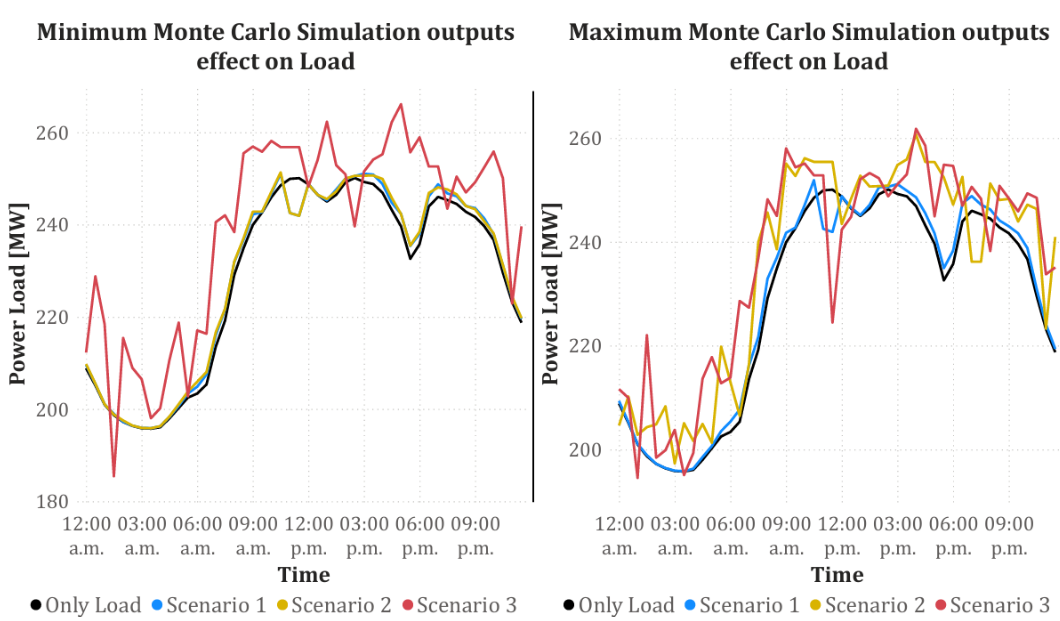

Figure 6. Power System Load per MCS output and scenario

Similarly, the work in [6] focuses on integrating cost savings and efficiency in electric vehicle charging infrastructure. Research in [7] emphasizes the interaction between electric vehicles and various energy markets. The present study extends this line of work by incorporating an optimization framework that combines day-ahead and real-time market dynamics with battery cost modeling.

3.2. Centralized Electric Vehicle Charging Management

Network operators are required to run optimal power flow (OPF) analyses. Table 3 presents the corresponding results, where the presence of not supplied energy (NSE) indicates that the EVA must adjust its daily load schedule. Figure 7 (a) illustrates OPF outcomes: the maximum output from the MCS analysis under Scenario 1 is shown in blue, and the minimum output from Scenario 3 is shown in red. These results demonstrate that the impact on daily system operation is minimal under Scenario 1, reflecting low EV adoption. In contrast, Scenario 3 highlights the negative consequences of poor coordination between CEVCM and DEVCM. The power system performance for Scenario 3 also reveals three instances of NSE (marked in red) and an increase in system losses of up to 7.79% compared to the business-as-usual (BAU) case.

Study [1] tests the same three scenarios under both unregulated charging and a centralized electric vehicle charging management (CEVCM) approach. In the case of unregulated EV charging, the resulting non-supplied energy (NSE) is 0.5 MWh for Scenario 1, 0.62 MWh for Scenario 2, and 2.74 MWh for Scenario 3. In this research, the application of DEVCM resolves power system operation issues for Scenarios 1 and 2. However, in Scenario 3, due to limited EV availability and the absence of coordination, the decentralized model results in 7.44 MWh of NSE. This highlights the necessity of coordinated management for systems with 3,750 EVs or more. The following section analyzes the impact of this coordination on the model.

Table 3. Centralized optimal power flow performance per scenario and MCS output

Bar	Without	Scenario 1		Scenario 2		Scenario 3	
	Evs	Min MCS	Max. MCS	Min MCS	Max. MCS	Min MCS	Max. MCS
Energy demand [MWh]	5486.08	5506.98	5509.18	5511.28	5654.06	5742.52	5672.24
Peak load [MW]	250.11	251.04	251.89	251.31	260.68	266.09	261.79
power factor	0.91	0.91	0.91	0.91	0.9	0.9	0.9
Power supplied [MWh]	5737.52	5760.42	5762.92	5765.14	5923.42	6013.54	5942.28
Losses [MWh]	251.44	253.46	253.74	253.86	269.36	271.02	270.04
ENS [MWh]	0	0	0	0	0	7.44	1.54
Maximum NSP [MW]	0	0	0	0	0	7.23	3.1
NSP Slash [#]						14	14

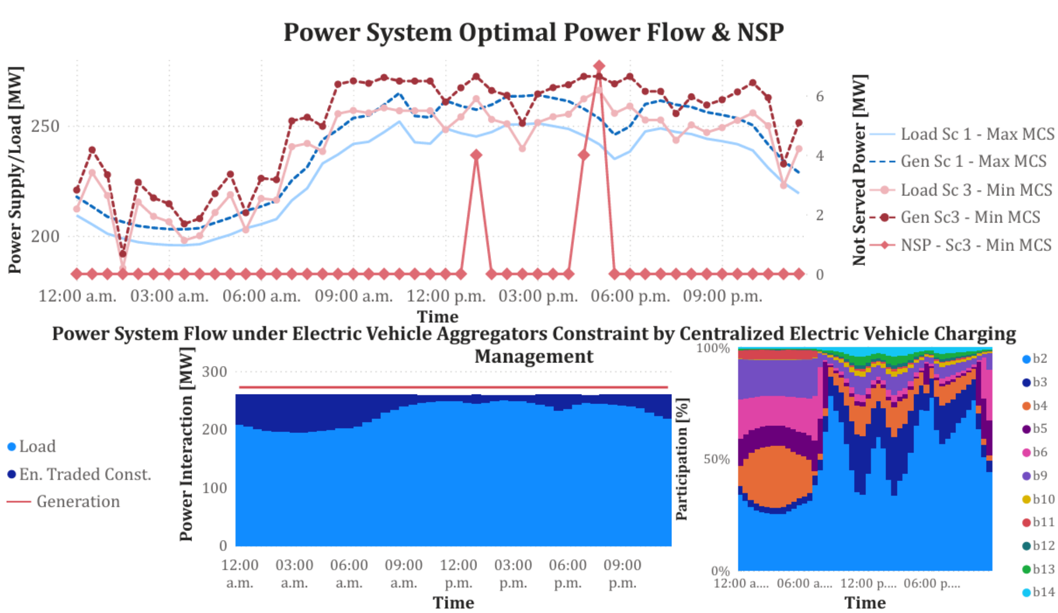

Figure 7. Power System operation performed by DNO

3.2.1. Coordination between centralized and decentralized management

The maximum amount of energy allowed for trading by each EVA serves as a constraint in the execution of decentralized charging management. Figure 7 (b) illustrates the energy trading limits established by distribution network operators (DNOs), while Figure 7 (c) shows the participation of each aggregator within those limits.

Scenario 3 is re-executed with these constraints applied to the EVAs. Table 4 presents the resulting energy traded between the aggregators and the DNO. Under this coordinated strategy, the DEVCM shifts battery charging to off-peak hours and maintains stability during peak demand periods. Figure 8 displays the response of the EVAs under these operating conditions, showing the minimum output in blue and the maximum output in red.

Table 4. Daily energy traded with the power system by EVA

Scenario 3	PEM [MWh]	
CR bar	min MCS	max MCS
2	74.891	71.135
3	12.277	10.419
4	30.783	2.248
5	30.180	18.688
6	14.582	19.129
9	22.681	30.668
10	2.992	3.092
11	7.193	7.663
12	2.468	4.367
13	4.257	5.713
14	3.714	7.084

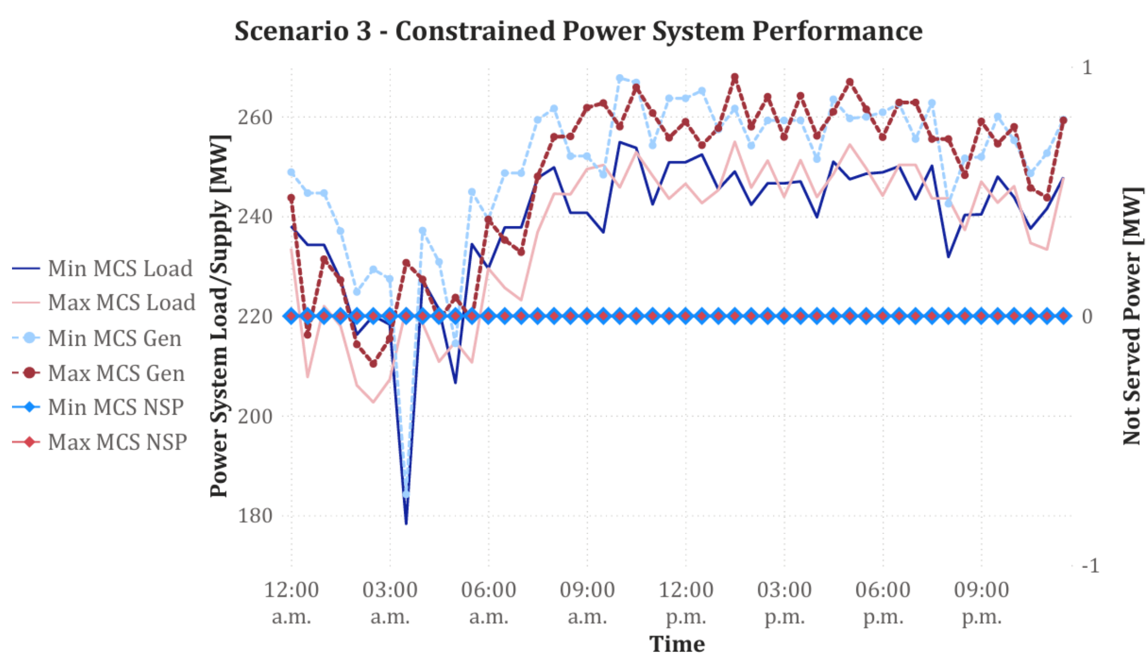

Figure 8. CEVCM coordination over DEVCM

For both MCS outputs under DNOs load regulation,no non-supplied energy (NSE) is observed, ensuring the system operates under normal conditions as long as the required energy transfer is achieved. The increase in charging activity may raise daily energy losses–up to 7.34% (shown in blue) and, to a lesser extent, up to 5.9% (shown in red). Power system variability decreases throughout the day due to the application of DEVCM. As a result, DNOs must plan for this operational behavior in the long term, aiming to reduce future peak-hour costs through increased base generation capacity. According to the reviewed literature, this additional capacity could be provided by renewable sources such as wind, hydro, or geothermal energy. Table 5 presents the CEVCM power system performance results.

Study [21] reports a positive economic impact on EVA charging management in the absence of geographical uncertainty and under the analysis of travel patterns for 500 electric vehicles. Additionally, the numerical results in [23] demonstrate that, under the most environmentally favorable scenario, excluding certain electric vehicles from the optimization process reduces emissions by 7% compared to the base case–while still yielding the highest profits for the operator. Similarly, the results in [24] propose a coordinated optimal operation strategy for a 33-node test system, achieving a reduction in operational costs from 17.74% to 17.53% and a decrease in system losses ranging from 29.49% to 31.36%.

Table 5. Centralized managed optimal power flow performance

Daily charge	Without SV	Scenario 3 CR	
		min MCS	max MCS
Energy demand [MWh]	5486.08	5734.54	5683.06
Maximum load [MW]	250.11	254.87	254.93
load factor	0.91	0.94	0.93
Power supplied [MWh]	5737.52	6004.56	5949.34
Losses [MWh]	251.44	270.02	266.28
ENS [MWh]	0	0	0
Maximum NSP [MW]	0	0	0
bar		0	0

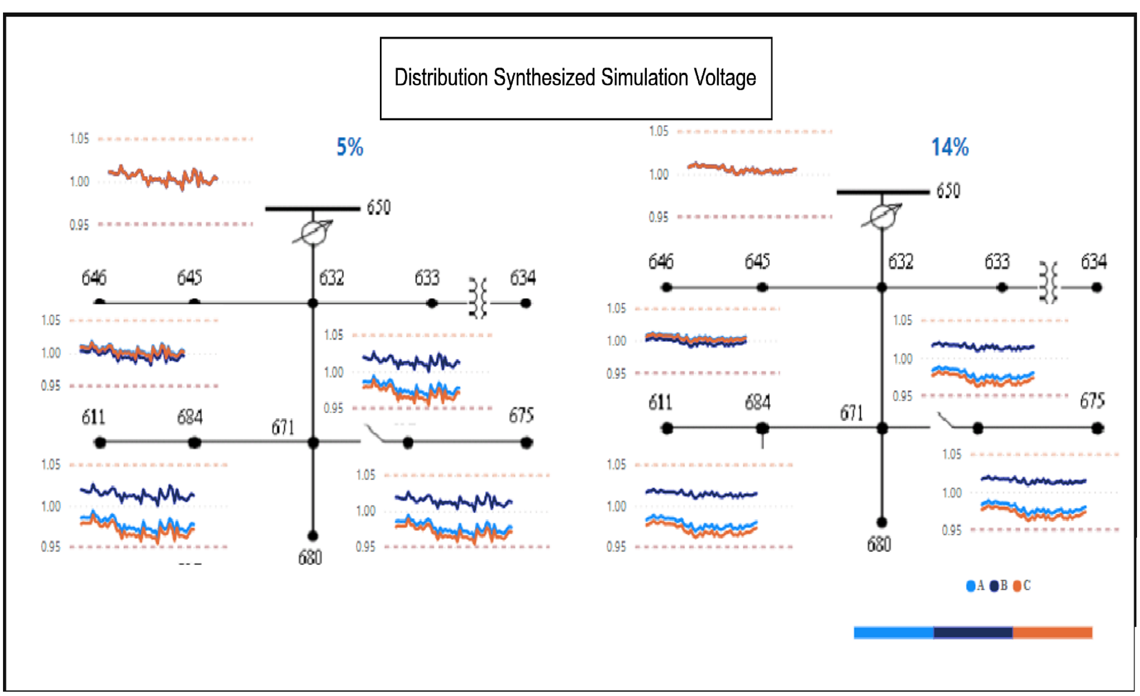

Figure 9. Distribution Power System (IEEE 13 bus) simulation

3.3. Distribution Analysis

Figure 9 presents the results for the 5% and 14% synthesized data sets, which showed the lowest error in the distribution analysis. The distribution network (DN) results reported in [1] indicate voltage levels approaching undervoltage conditions. In contrast, the findings of this study show that the voltage levels at the farthest buses (671, 675, 611, 684, 652, 680, and 692) are less prone to undervoltageissues.

4. Conclusions

The integration of decentralized electric vehicle charging management (DEVCM) into the transmission power system (PS) improves its operational performance compared to unregulated charging, as reported in [1] and illustrated inTable 3, Figure 6, and Figure 7. Under purely decentralized management, the power system performs well in Scenarios 1 and 2, even under maximum MCS outputs, without the need for additional energy management policies. However, Scenario 3–with higher EV penetration–demands additional policy interventions to maintain system stability.

This research introduces a novel Centralized Electric Vehicle Charging Management (CEVCM) system that operates independently of external influences, ensuring reliable and predictable EV charging behavior. By reducing stress on the power grid, it contributes to mitigating power outages and related safety risks. Moreover, CEVCM infrastructure can be deployed in phases, adapting to EV penetration rates and enabling geographically targeted placement based on observed travel patterns. As demonstrated in Table 5 and Figure 8, the CEVCM approach improves the daily operational performance of the power system.

This work also provides a valuable framework for addressing coordination challenges in current distributed energy management policies. The CEVCM model supports data-driven planning for charging environments, guided by actual EV usage behavior. This facilitates the optimization of power system infrastructure near substations experiencing high EV adoption but limited energy trading activity, as shown in Figure 7. Furthermore, this study evaluates the unbalanced IEEE 13-bus power system as a distribution network. The model demonstrates compliance with Peruvian voltage regulations, even at the most remote buses of the distribution system.

For future research, the proposed model, particularly the version incorporating the non-supplied energy (NSE) variable, offers significant potential for evaluating grid expansion needs associated with the integration of distributed renewable energy sources. Further studies could explore combining the CEVCM framework with centralized coordination mechanisms and EV-based generation planning. The data synthesis process could also be refined to focus on a targeted set of operational and contingency scenarios, thereby reducing computational complexity. Finally, a hybrid charging management approach that integrates both controlled and uncontrolled strategies, including day-ahead coordination, distributed generation, and real-time aggregator flexibility (e.g., demand response, EV battery state-of-charge control, and distributed generation management), may yield additional operational benefits.

Acknowledgments

The authors gratefully acknowledge the support of the "Program of Doctorates in Peruvian Universities," promoted by the Ministry of Education (MINEDU), the National Council of Science, Technology and Technological Innovation (CONCYTEC), and the National Fund for Scientific, Technological and Technological Innovation Development (FONDECYT).

Contributor Roles

- **Carlos W. Villanueva-Machado:** Conceptualization, data curation, formal analysis, investigation, methodology, software, visualization, writing – original draft, writing – review and editing.
- **Jaime E. Luyo:** Formal analysis, investigation, project administration, supervision, validation.
- **Alberto Rios-Villacorta:** Formal analysis, investigation, project administration, supervision, validation.

References

[1] C. W. Villanueva-Machado, J. E. Luyo, and A. Ríos-Villacorta, "Impacto de la simulación montecarlo de carga no controlada de vehículos eléctricos en la generación distribuida," *Ingenius*, no. 30, pp. 120–134, Jul. 2023. [Online]. Available: https://doi.org/10.17163/ings.n30.2023.10

[2] S. Li, P. Zhao, C. Gu, J. Li, S. Cheng, and M. Xu, "Battery protective electric vehicle charging management in renewable energy system," *IEEE Transactions on Industrial Informatics*, vol. 19, no. 2, pp. 1312–1321, Feb. 2023. [Online]. Available: https://doi.org/10.1109/TII.2022.3184398

[3] Y. Yang, Q.-S. Jia, G. Deconinck, X. Guan, Z. Qiu, and Z. Hu, "Distributed coordination of EV charging with renewable energy in a microgrid of buildings," *IEEE Transactions on Smart Grid*, vol. 9, no. 6, pp.

6253–6264, Nov. 2018. [Online]. Available: https://doi.org/10.1109/TSG.2017.2707103

[4] A. J. Cheng, B. Tarroja, B. Shaffer, and S. Samuelsen, "Comparing the emissions benefits of centralized vs. decentralized electric vehicle smart charging approaches: A case study of the year 2030 California electric grid," *Journal of Power Sources*, vol. 401, pp. 175–185, Oct. 2018. [Online]. Available: https://doi.org/10.1016/j.jpowsour.2018.08.092

[5] S. Zeynali, N. Rostami, A. Ahmadian, and A. Elkamel, "Two-stage stochastic home energy management strategy considering electric vehicle and battery energy storage system: An ann-based scenario generation methodology," *Sustainable Energy Technologies and Assessments*, vol. 39, p. 100722, Jun. 2020. [Online]. Available: https://doi.org/10.1016/j.seta.2020.100722

[6] M. R. Sarker, H. Pandžić, K. Sun, and M. A. Ortega-Vázquez, "Optimal operation of aggregated electric vehicle charging stations coupled with energy storage," *IET Generation, Transmission & Distribution*, vol. 12, no. 5, pp. 1127–1136, Jan. 2018. [Online]. Available: https://doi.org/10.1049/iet-gtd.2017.0134

[7] M. R. Sarker, Y. Dvorkin, and M. A. Ortega-Vázquez, "Optimal participation of an electric vehicle aggregator in day-ahead energy and reserve markets," *IEEE Transactions on Power Systems*, vol. 31, no. 5, pp. 3506–3515, Sep. 2016. [Online]. Available: https://doi.org/10.1109/TPWRS.2015.2496551

[8] H. Kikusato, K. Mori, S. Yoshizawa, Y. Fujimoto, H. Asano, Y. Hayashi, A. Kawashima, S. Inagaki, and T. Suzuki, "Electric vehicle charge–discharge management for utilization of photovoltaic by coordination between home and grid energy management systems," *IEEE Transactions on Smart Grid*, vol. 10, no. 3, pp. 3186–3197, May 2019. [Online]. Available: http://dx.doi.org/10.1109/TSG.2018.2820026

[9] M. F. Shaaban, M. Ismail, E. F. El-Saadany, and W. Zhuang, "Real-time pev charging/discharging coordination in smart distribution systems," *IEEE Transactions on Smart Grid*, vol. 5, no. 4, pp. 1797–1807, Jul. 2014. [Online]. Available: http://dx.doi.org/10.1109/TSG.2014.2311457

[10] M. M. Hoque, M. Khorasany, R. Razzaghi, H. Wang, and M. Jalili, "Transactive coordination of electric vehicles with voltage control in distribution networks," *IEEE Transactions on Sustainable Energy*, vol. 13, no. 1, pp. 391–402, Jan. 2022. [Online]. Available: https://doi.org/10.1109/TSTE.2021.3113614

[11] N. Rahbari-Asr and M.-Y. Chow, "Cooperative distributed demand management for community charging of PHEV/PEVs based on KKT conditions and consensus networks," *IEEE Transactions on Industrial Informatics*, vol. 10, no. 3, pp. 1907–1916, Aug. 2014. [Online]. Available: https://doi.org/10.1109/TII.2014.2304412

[12] D. Said and H. T. Mouftah, "A novel electric vehicles charging/discharging management protocol based on queuing model," *IEEE Transactions on Intelligent Vehicles*, vol. 5, no. 1, pp. 100–111, Mar. 2020. [Online]. Available: https://doi.org/10.1109/TIV.2019.2955370

[13] X. Yang, C. Xu, Y. Zhang, W. Yao, J. Wen, and S. Cheng, "Real-time coordinated scheduling for ADNs with soft open points and charging stations," *IEEE Transactions on Power Systems*, vol. 36, no. 6, pp. 5486–5499, Nov. 2021. [Online]. Available: https://doi.org/10.1109/TPWRS.2021.3070036

[14] M. Shafie-Khah, P. Siano, D. Z. Fitiwi, N. Mahmoudi, and J. P. S. Catalao, "An innovative two-level model for electric vehicle parking lots in distribution systems with renewable energy," *IEEE Transactions on Smart Grid*, vol. 9, no. 2, pp. 1506–1520, Mar. 2018. [Online]. Available: https://doi.org/10.1109/TSG.2017.2715259

[15] M. Mohiti, H. Monsef, and H. Lesani, "A decentralized robust model for coordinated operation of smart distribution network and electric vehicle aggregators," *International Journal of Electrical Power & Energy Systems*, vol. 104, pp. 853–867, Jan. 2019. [Online]. Available: https://doi.org/10.1016/j.ijepes.2018.07.054

[16] M. S. H. Nizami, M. J. Hossain, and K. Mahmud, "A coordinated electric vehicle management system for grid-support services in residential networks," *IEEE Systems Journal*, vol. 15, no. 2, pp. 2066–2077, Jun. 2021. [Online]. Available: https://doi.org/10.1109/JSYST.2020.3006848

[17] F. L. Da Silva, C. E. H. Nishida, D. M. Roijers, and A. H. Reali Costa, "Coordination of electric vehicle charging through multiagent reinforcement learning," *IEEE Transactions on Smart Grid*, vol. 11, no. 3, pp. 2347–2356, May 2020. [Online]. Available: https://doi.org/10.1109/TSG.2019.2952331

[18] S. Deilami, A. S. Masoum, P. S. Moses, and M. A. S. Masoum, "Real-time coordination of plug-in electric vehicle charging in smart grids

to minimize power losses and improve voltage profile," *IEEE Transactions on Smart Grid*, vol. 2, no. 3, pp. 456–467, Sep. 2011. [Online]. Available: https://doi.org/10.1109/TSG.2011.2159816

[19] J. Hu, S. You, M. Lind, and J. Ostergaard, "Coordinated charging of electric vehicles for congestion prevention in the distribution grid," *IEEE Transactions on Smart Grid*, vol. 5, no. 2, pp. 703–711, Mar. 2014. [Online]. Available: https://doi.org/10.1109/TSG.2013.2279007

[20] M. R. Sarker, M. A. Ortega-Vázquez, and D. S. Kirschen, "Optimal coordination and scheduling of demand response via monetary incentives," *IEEE Transactions on Smart Grid*, vol. 6, no. 3, pp. 1341–1352, May 2015. [Online]. Available: https://doi.org/10.1109/TSG.2014.2375067

[21] J. Luyo, C. Villanueva, A. Delgado, and C. Carbajal, "Electric vehicles aggregator participation in energy markets considering uncertainty travel patterns," *International Journal of Innovative Technology and Exploring Engineering*, vol. 8, no. 12, pp. 4994–4998, Oct. 2019. [Online]. Available: http://dx.doi.org/10.35940/ijitee.L3747.1081219

[22] P. Harsh and D. Das, "Optimal coordination strategy of demand response and electric vehicle aggregators for the energy management of reconfigured grid-connected microgrid," *Renewable and Sustainable Energy Reviews*, vol. 160, p. 112251, May 2022. [Online]. Available: https://doi.org/10.1016/j.rser.2022.112251

[23] W. Yang, J. Guo, and A. Vartosh, "Retracted: Optimal economic-emission planning of multi-energy systems integrated electric vehicles with modified group search optimization," *Applied Energy*, vol. 311, p. 118634, Apr. 2022. [Online]. Available: https://doi.org/10.1016/j.apenergy.2022.118634

[24] S. Gupta, A. Maulik, D. Das, and A. Singh, "Coordinated stochastic optimal energy management of grid-connected microgrids considering demand response, plug-in hybrid electric vehicles, and smart transformers," *Renewable and Sustainable Energy Reviews*, vol. 155, p. 111861, Mar. 2022. [Online]. Available: https://doi.org/10.1016/j.rser.2021.111861

[25] A. Najafi, M. Pourakbari-Kasmaei, M. Jasinski, M. Lehtonen, and Z. Leonowicz, "A hybrid decentralized stochastic-robust model for optimal coordination of electric vehicle aggregator and energy hub entities," *Applied Energy*, vol. 304, p. 117708, Dec. 2021. [Online]. Available: https://doi.org/10.1016/j.apenergy.2021.117708

[26] EV Volumes. (2023) Global EV sales for 2023. EV Volumes Autovista Group. [Online]. Available: https://upsalesiana.ec/ing34ar4r26

[27] PNUMA, *Movilidad eléctrica: Avances 19 en América Latina y el Caribe 2019*. Programa de las Naciones Unidas para el Medioambiente, 2019. [Online]. Available: https://upsalesiana.ec/ing34ar4r27

[28] LNE. (2023) Aumentó la penetración de vehículos eléctricos e híbridos en América Latina durante el 2022. La nota económica. [Online]. Available: https://upsalesiana.ec/ing34ar4r28

[29] MOVELATAM, *Interoperability for recharging electric vehicles in Latin America and the Caribbean, practical guide of recommendations*. United Nations Environment Programme, 2022. [Online]. Available: https://upsalesiana.ec/ing34ar4r29

[30] AAP. (2019) Los protagonistas de la nueva era automotriz: Vehículos eléctricos e hibrídos en el perú. Asociación Automotríz del Perú. [Online]. Available: https://upsalesiana.ec/ing34ar4r30

[31] C. W. Villanueva. (2024) Operative analysis of electric vehicle controlled charging management: Centralized - decentralized coordination. Git-Hub. Inc. [Online]. Available: https://upsalesiana.ec/ing34ar4r37

[32] L. Wang, S. Sharkh, and A. Chipperfield, "Optimal decentralized coordination of electric vehicles and renewable generators in a distribution network using A* search," *International Journal of Electrical Power & Energy Systems*, vol. 98, pp. 474–487, Jun. 2018. [Online]. Available: https://doi.org/10.1016/j.ijepes.2017.11.036

[33] S. Pirouzi, J. Aghaei, T. Niknam, H. Farahmand, and M. Korpas, "Exploring prospective benefits of electric vehicles for optimal energy conditioning in distribution networks," *Energy*, vol. 157, pp. 679–689, Aug. 2018. [Online]. Available: https://doi.org/10.1016/j.energy.2018.05.195

[34] J. Czyzyk, M. Mesnier, and J. More, "The neos server," *IEEE Computational Science and Engineering*, vol. 5, no. 3, pp. 68–75, 1998. [Online]. Available: https://doi.org/10.1109/99.714603

[35] E. D. Dolan, *NEOS server 4.0 administrative guide.*, Jul. 2001. [Online]. Available: http://dx.doi.org/10.2172/822567

[36] W. Gropp and J. J. More, "Optimization environments and the NEOS server," in *Conference: 3. International Workshop on short*

term experiments under strongly reduced gravity conditions, Bremen (Germany), 8-11 Jul 1996. Argonne National Lab. (ANL), Argonne, IL (United States), 03 1997. [Online]. Available: https://upsalesiana.ec/ing34ar4r35

[37] PSCAD. (2018) IEEE 14 bus system. Manitoba Hydro International Ltd. [Online]. Available: https://upsalesiana.ec/ing34ar4r36